Soft X-ray Emission Spectra of Capillary Plasma

VRBA Pavel, JANČÁREK Alexander[1], VRBOVÁ Miroslava[1], SCHOLZOVÁ Lenka[1],
FOJTÍK Anton[1], TAMÁŠ Martin[1] and HAVLÍKOVÁ Radka[1]

Institute of Plasma Physics, AS CR, CZ-18221 Prague 8, Czech Republic
[1]Czech Technical University, Břehová 7, CZ-115 19 Prague 1, Czech Republic

Abstract

Experimental and computer study of plasma, created in initially evacuated polyacethal and polyethylene capillary, is reported here. Soft X-ray spectroscopy was used as the diagnostic tool. The time-integrated spectra of plasma measured correspond to the computer simulated spectra as provided by the NPINCH and FLY codes.

Keywords:

1. Introduction

Non-stationary plasma of a fast capillary electrical discharge was studied as a potential active medium for a soft X-ray laser. We aim to achieve lasing at 18.2 nm wavelength with hydrogen-like carbon ions C^{5+} in polyacethal or polyethylene plasma [1]. In order to obtain conditions favourable for three-body recombination pumping, the capillary pulse plasma should be heated initially as the carbon ions have to be fully ionized. During the next stage, the plasma electrons should be cooled quickly. Details of the capillary plasma evolution and ion energy level populations are evaluated by means of MHD (magnetohydrodynamic) plasma modelling and by ion kinetic post-processor evaluations. Experimental time-integrated soft X-ray spectra and calculated ones are compared in this contribution.

2. Experiment
2.1 Experimental setup

Polyacethal and polyethylene, 5 cm long capillaries each with 1.1 mm diameter were used in our experiments. The pumping energy is stored in a bank of 24 ceramic capacitors of 15.3 nF total capacity that are mounted in parallel around the capillary between two circular flat plates providing a low inductance. The applied voltage maximum is 40 kV, so up to 12 J energy can be stored and subsequently drained into the capillary. The main discharge is triggered by a spark between coaxial electrodes (see Fig. 1). As the discharge plasma column resistance decreases very quickly and its value becomes less than 1 Ω, the discharge circuit may be described as an under-dumped resonant RLC series circuit with quasi-period about 260 ns. The current peak value I_{max} is 10 kA.
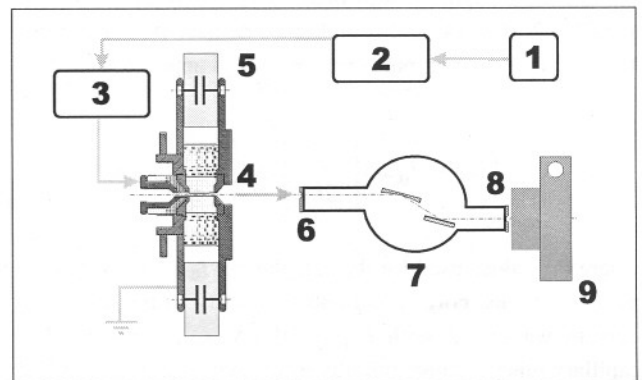

Fig. 1 Experimental set up: 1-Manual trigger, 2-Pulse generator, 3-High voltage pulser, 4-Capillary, 5-Capacitor bank, 6-Entrance slit of the monochromator, 7- Monochromator, 8-Exit slit of the monochromator, 9-CCD camera.

Time integrated emission spectra in the 10–26 nm wavelength region are measured with the JOBIN YVON monochromator PGM-PGS 200, output slit energy of which is recorded by the Reflex, Ltd. BICCD camera RXBIC 512c for each shot separately. The two-dimensional image of the monochromator exit slit, as recorded and stored in a computer, provides wavelength resolution of 0.11 nm. The spectral energies are determined for various wavelengths with 0.02 nm step. The time integrated spectra are obtained by a simple processing of the stored data. Each spectral point on figures presented here is an average of at least five subsequent shots data.

Corresponding author's e-mail: vrba@ipp.cas.cz

2.2 Time integrated spectra

The emission spectra of plasma generated in polyacethal $(CH_2O)_n$ and polyethylene $(CH_2)_n$ capillary are depicted at Fig. 2 (a), (b). In the selected spectral range, only the lines corresponding to both carbon and oxygen ions with the ionization degree $Z > 3$ may be found. If the polyacethal capillary is used, the spectral lines of O^{4+} and O^{5+} are dominant. When comparing these results with the measurements of Gotou *et al.* [2], although done under slightly different experimental conditions, a good agreement can be seen. With polyethylene capillary, the identified spectral lines correspond namely to C^{3+} and C^{4+} ions. Experimental conditions for both types of capillaries were the same. The dominant oxygen line intensities measured with the polyacethal capillary are stronger than the dominant carbon lines observed in the case of polyethylene one.

3. Computer simulations
3.1 Magnetohydrodynamics

Capillary discharge plasma quantities were calculated by means of NPINCH code under the one-dimensional, two-temperature, one-fluid MHD approximation [3]. The model considers the capillary wall material as a dense cold neutral gas ($Z = 7$, $A = 14$, and initial mass density $\rho_0 = 1$ g/cm³). The electrical current pulse time profile is approximated by

$$I(t) = I_0 \sin\left(\frac{\pi t}{2t_0}\right)\exp\left(-\frac{t}{t_1}\right),$$

where the values used for the calculation: $I_0 = 14$ kA, $t_0 = 66$ ns, $t_1 = 150$ ns, correspond approximately to the measured current waveform with $I_{max} = 10$ kA, $t_{max} = 54$ ns. The capillary inner volume, initially evacuated, is gradually filled by a material ablated from the wall. Resulting time-profiles of the electron density and electron & ion temperature axial values are on Fig. 3. The first axial electron density peak (at $N_e = 2\times10^{18}$ cm⁻³, $t = 20$ ns) corresponds to a quick compression of the plasma created during the leading current pulse edge. The plasma electron temperature T_e is increasing here due to the increasing local current density. Its peak value about $T_e = 130$ eV is reached at $t_{max} = 40$ ns. Relatively quick plasma cooling at the end of the first current half period is caused by the cool plasma coming from the wall. In the current second half period the axial plasma is relatively cold, $T_e \leq 20$ eV, and axial electron density grows due to the wall ablation all the time.

3.2 Ion population density time dependences

The temporal history of the axial plasma electron density and temperature, as obtained from MHD simulations (Fig. 3), were used as input data for the FLY code [4]. Resulting time profiles of the ionization fractions and energy level population for lithium-, helium- and hydrogen-like carbon and oxygen ions are presented on Fig. 4. During the whole current quasi-period (i.e. on the time interval 0–260 ns) carbon ions C^{4+},
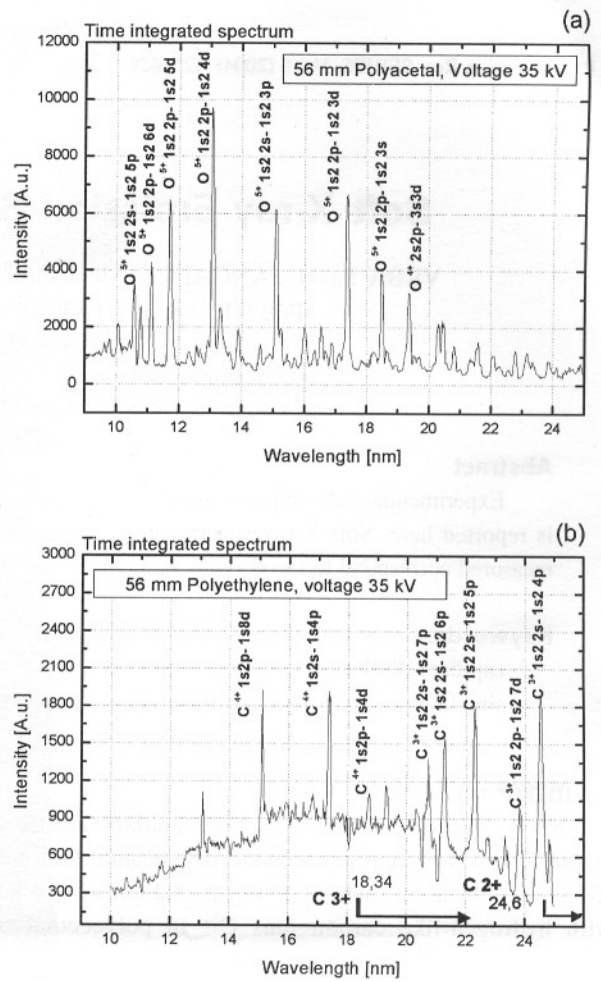

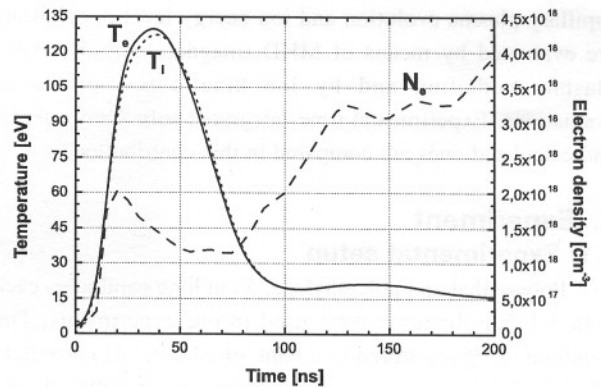Fig. 2 Time-integrated spectra emitted from (a) polyacethal, (b) polyethylene capillary discharge.

Fig. 3 Calculated time dependences of axial plasma electron density N_e, electron and ion temperatures T_e, and T_i.

C^{5+} and oxygen ions O^{5+}, O^{6+} are dominating. The hydrogen-like ion C^{5+} concentration prevails on the interval of 25 to 90 ns. Concentration of the fully stripped ion, C^{6+}, is negligible during all that time. Time dependence of the hydrogen-like carbon ion energy levels population (see Fig. 4b) provides evidence of a population inversion on the Balmer α transition starting at 76 ns. Unfortunately, the absolute value of the
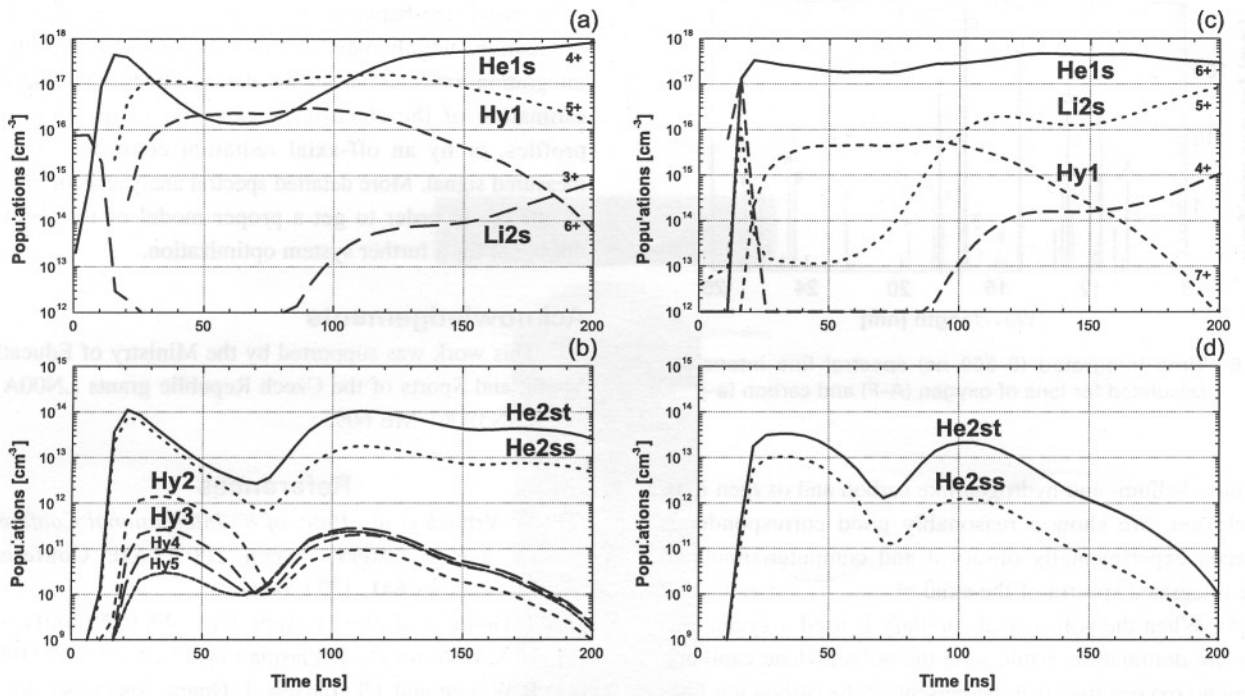

Fig. 4   Time dependences of population densities of (a) carbon ions, (b) excited states of helium- and hydrogen- like carbon ions, (c) oxygen ions, (d) selected excited states of helium- like oxygen ions.

Table 1   Identification of spectral lines in the evaluated time integrated spectra (see Fig. 5)

Label	Wavelength [nm]	Ion	Configuration	g_i	g_k	A_{ki} [s^{-1}]
A	10.48	O^{5+}	1s^{2}2s-1s^{2}5p	2	6	6.48×10^9
B	11.58	O^{5+}	1s^{2}2s-1s^{2}4p	2	6	1.23×10^{10}
C	12.98	O^{5+}	1s^{2}2p-1s^{2}4d	6	10	2.91×10^{10}
D	15.01	O^{5+}	1s^{2}2s-1s^{2}3p	2	6	2.62×10^{10}
E	17.31	O^{5+}	1s^{2}2p-1s^{2}3d	6	10	8.78×10^{10}
F	18.41	O^{5+}	1s^{2}2p-1s^{2}3s	6	2	1.71×10^{10}
a	15.84	C^{4+}	1s2s-1s6p	1	3	1.75×10^9
b	16.73	C^{4+}	1s2p-1s5d	9	15	6.56×10^9
c	18.23	C^{5+}	2-3	8	18	5.72×10^{10}
d	18.64	C^{4+}	1s2s-1s4p	1	3	5.77×10^9
e	19.67	C^{3+}	1s^{2}2s-1s^{2}12p	2	6	8.96×10^7
f	22.34	C^{3+}	1s^{2}2s-1s^{2}5p	2	8	1.21×10^9
g	24.49	C^{3+}	1s^{2}2s-1s^{2}4p	2	6	2.27×10^9
h	24.75	C^{4+}	1s2s-1s3p	1	3	1.28×10^{10}
i	25.95	C^{3+}	1s^{2}2p-1s^{2}5d	6	10	2.73×10^9
j	26.60	C^{4+}	1s2p-1s3d	3	5	3.95×10^{10}

hydrogen-like carbon ions density is too low to get detectable gain factor.

3.3 Time-integrated spectra

Using the subprogram FLYSPEC we evaluated time integrated (0–500 ns) emission spectra for the 8–28 nm wavelength interval (see Fig. 5). The oxygen and carbon ion spectral lines are denoted by the capital and small letters, respectively. Corresponding identification of spectral lines is

seen from Table 1. The strongest spectral lines in the range of 8–18 nm belong to O^{4+} and O^{5+} ions. The spectral lines of carbon ions C^{3+}, C^{4+}, and C^{5+} are less intensive, but dominating in the range 18–25 nm.

4. Conclusions

In the soft X-ray spectral region studied in this work, only the spectral lines of C^{3+}, C^{4+}, and C^{5+} ions may be essentially found. Consequently, the FLY code that deals with
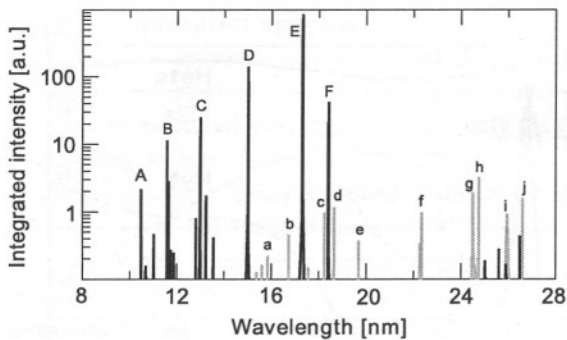
Fig. 5   Time integrated (0–500 ns) spectral line intensities calculated for ions of oxygen (A–F) and carbon (a–j).

lithium-, helium- and hydrogen-like carbon and oxygen ions, is relevant. We show a reasonably good correspondence between experimentally observed and computer-simulated time-integrated spectra of the axial plasma (compare Figs. 2 and 5). When the polyacethal capillary is used, oxygen ions lines are dominating, while with the polyethylene capillary, where no oxygen ions may be presented, the carbon ion lines are identified, but all are less intense. There is no full correspondence between the calculated and measured line intensities, which may be caused either by the shorter integration time interval in simulations, or by the inaccurate estimation of the electron density and temperature axial profiles, or by an off-axial radiation contribution to the measured signal. More detailed spectral analysis is in progress in our lab in order to get a proper model of the capillary discharge for a further system optimization.

Acknowledgements

References

[1]   M. Vrbová *et al.*, *Proc. of 8th International Conference on X-Ray Lasers*, Aspen 2002, AIP Conference Proceedings **641**, 139 (2002).

[2]   T. Gotou *et al.*, Jpn. J. Appl. Phys. **40**, 995 (2001).

[3]   N.A. Bobrova *et al.*, Plasma Phys. Rep. **22**, 387 (1996).

[4]   R.W. Lee and J.T. Larsen, J. Quant. Spectrosc. Radiat. Transfer **56**, 535 (1996).